

Melatonin protects rat cerebellar granule cells against electromagnetic field-induced increases in Na⁺ currents through intracellular Ca²⁺ release

Dong-Dong Liu, Zhen Ren, Guang Yang, Qian-Ru Zhao, Yan-Ai Mei *

School of Life Sciences, Institutes of Brain Science and State Key Laboratory of Medical Neurobiology, Fudan University, Shanghai, China

Received: August 27, 2013; Accepted: January 18, 2014

Abstract

Although melatonin (MT) has been reported to protect cells against oxidative damage induced by electromagnetic radiation, few reports have addressed whether there are other protective mechanisms. Here, we investigated the effects of MT on extremely low-frequency electromagnetic field (ELF-EMF)-induced Na_v activity in rat cerebellar granule cells (GCs). Exposing cerebellar GCs to ELF-EMF for 60 min. significantly increased the Na_v current (*I*_{Na}) densities by 62.5%. MT (5 μM) inhibited the ELF-EMF-induced *I*_{Na} increase. This inhibitory effect of MT is mimicked by an MT₂ receptor agonist and was eliminated by an MT₂ receptor antagonist. The Na_v channel steady-state activation curve was significantly shifted towards hyperpolarization by ELF-EMF stimulation but remained unchanged by MT in cerebellar GC that were either exposed or not exposed to ELF-EMF. ELF-EMF exposure significantly increased the intracellular levels of phosphorylated PKA in cerebellar GCs, and both MT and IIK-7 did not reduce the ELF-EMF-induced increase in phosphorylated PKA. The inhibitory effects of MT on ELF-EMF-induced Na_v activity was greatly reduced by the calmodulin inhibitor KN93. Calcium imaging showed that MT did not increase the basal intracellular Ca²⁺ level, but it significantly elevated the intracellular Ca²⁺ level evoked by the high K⁺ stimulation in cerebellar GC that were either exposed or not exposed to ELF-EMF. In the presence of ruthenium red, a ryanodine-sensitive receptor blocker, the MT-induced increase in intracellular calcium levels was reduced. Our data show for the first time that MT protects against neuronal *I*_{Na} that result from ELF-EMF exposure through Ca²⁺ influx-induced Ca²⁺ release.

Keywords: melatonin • ELF-EMF • Na⁺ currents • Ca²⁺ release • cerebellar granule cells

Introduction

Several studies have noted that exposure to extremely low-frequency electromagnetic fields (ELF-EMF) alters animal behaviours and causes biological effects, including changes in gene expression, the regulation of cell survival and the promotion of cell differentiation [1–3]. In addition, exposure to EMF induces changes in cerebral blood flow in old Alzheimer's mice [4]. Enzyme activity in cytosol or at the membrane and subsequent alterations in intracellular signalling are found in lymphoma B cells and Chinese hamster lung cells upon exposure to ELF-EMF [5, 6]. Extremely low-frequency electromag-

netic fields can also modify the biophysical properties of cell membranes as shown by changes in the membrane permeability of carbonic anhydrase [7] and stimulation of the activity of Ca²⁺-activated potassium channels *via* increases in Ca²⁺ concentration and voltage-gated calcium channels [3, 8, 9]. We recently reported that ELF-EMF exposure significantly activated the voltage-gated sodium (Na_v) channels of cerebellar GCs [10]. This activation is mediated by an increase in the intracellular concentration of arachidonic acid and involves EP receptor-mediated activation of the cAMP/PKA signalling pathway [10].

Melatonin (MT), which is synthesized and primarily secreted by the pineal gland, participates in many important physiological functions, including the control of seasonal reproduction, and influences the immune system and circadian rhythms [11, 12]. *In vitro* and *in vivo* studies have revealed that MT and its metabolites can reduce oxidative stress-induced damage to proteins, lipids and nucleic acids in the presence of free radicals because of its free radical-scavenging

*Correspondence to: Dr. Mei YAN-AI, School of Life Sciences, Institute of Brain Science, Fudan University, Shanghai 200433, China. Tel.: +86-21-55664711 Fax: +86-21-65650149 E-mail: yamei@fudan.edu.cn

properties [13–15]. Because it has been postulated that EMF exposure can affect the function of biological systems by inducing oxidative damage, the effects of MT on EMF-induced oxidative damage, cancer risk and neurodegeneration have been investigated [16, 17]. Besides its direct free radical-scavenging properties, MT has been shown to modulate apoptosis caused by wireless (2.45 GHz)-induced oxidative stress through cation channels, such as transient receptor potential (TRP) and voltage-gated Ca^{2+} channels in neurons and transfected cells [18, 19]. In addition, MT modulates the delay in outward rectifying K^+ channels resulting in the promotion of cerebellar GC migration or the protection of cerebellar GCs against apoptosis [20, 21]. However, there have been relatively few studies concerning the effect of MT on Na^+ channels, especially EMF-induced Na^+ channels activity.

Voltage-gated sodium channels are one of the primary classes of ion channels responsible for driving neuronal excitability in both the central and the peripheral nervous system. Voltage-gated sodium channels are clinically important because they play an important role in the generation of neuronal activity, and alterations in Na_v channels are key factors in a number of pathologies [22]. Previous studies from other groups have revealed that Na_v channels participate in the rising phase of the neuronal action potential and contribute to many cellular functions, including apoptosis, motility and secretory membrane activity [22, 23]. Moreover, EMF exposure was recently reported to modulate neuronal excitation and neurogenesis, which may be related to Na_v channel activity [24, 25]. Our previous data have demonstrated that ELF-EMF exposure significantly activates the Na_v channels of cerebellar GCs, which might be an important effect of EMF on neuronal excitation in the cerebellar GCs. Thus, a thorough investigation of the influence of ELF-EMF on Na_v channels and the corresponding mechanism of action could elucidate the ELF-EMF-induced biological effects on brain physiology, pathogenesis and neural development. Therefore, it is interesting to address whether MT can modulate ELF-EMF-induced Na_v channel activity.

This study was conducted to determine whether MT influences the Na^+ channels of cerebellar GCs exposed to ELF-EMF and, if so, whether this effect is mediated by inactivation of the cAMP/PKA signalling pathway. The data presented in this report demonstrate that the activity of neuronal Na^+ channels by ELF-EMF stimulation is significantly reversed by MT. Notably, the effect of MT on ELF-EMF-induced Na^+ is not mediated by inhibition of the cAMP/PKA signalling pathway but by increasing intracellular calcium levels.

Materials and methods

Ethics statement

This study was carried out in strict accordance with the recommendations in the Guide for the Care and Use of Laboratory Animals of the National Institutes of Health. The protocol was approved by the Committee on the Ethics of Animal Experiments of Fudan University (Permit Number: 20090614-001). All surgery was performed under sodium pentobarbital anaesthesia, and all efforts were made to minimize suffering.

Primary cell culture

Cells were derived from the cerebellum of 7-day-old Sprague–Dawley rat pups as described previously [26]. Isolated cells were then plated onto 35-mm-diameter Petri dishes coated with poly-L-lysine (1 $\mu\text{g}/\text{ml}$) at a density of $2.5 \times 10^5/\text{cm}^2$. Cultured cells were incubated at 37°C with 5% CO_2 in DMEM supplemented with 10% foetal calf serum, glutamine (5 mM), insulin (5 $\mu\text{g}/\text{ml}$), KCl (25 mM) and 1% antibiotic-antimycotic solution. All experiments were carried out with cerebellar GCs grown for 6–8 days in culture (DIC). For Ca^{2+} imaging experiments, the cells were plated onto poly-L-lysine-coated glass coverslips (12 mm in diameter).

Electromagnetic field production

The system used to expose cerebellar GCs cells to electromagnetic fields was the same as that used in previous studies, with some revisions (I-ONE, Shanghai, China) [27, 28]. Briefly, a 50-Hz magnetic field was generated by a pair of Helmholtz coils placed in opposition to each other. The coils were powered by a generator system that produced sinusoidal input voltage, and the magnetic flux densities could be regulated within the range of 0–1.0 mT. The device was powered by an AC power generator, and the EMF frequency and density were monitored by an EMF sensor that was connected to a digital multimeter. The geometry of the system assured a uniform field for the exposed cultured cells. The surfaces of the culture plates were parallel to the force lines of the alternating magnetic field in the solenoid. The air and culture medium temperatures were continuously monitored for the duration of experiments. The maximum temperature increase recorded in the cultures that were exposed to ELF-EMF (compared with non-exposed cultures) was $0.4 \pm 0.1^\circ\text{C}$. To identify any possible influence of this increase on our results, we compared data obtained from cerebellar GCs cultured in two different CO_2 incubators at temperature settings of 37.0 and 37.4°C, and the results were consistent. The incubator was kept closed throughout the EMF or non-EMF experiments to ensure that the conditions were stable. Non-EMF groups were incubated in the same incubator under the same conditions as those used for the exposed groups but without EMF.

Patch-clamp recordings

Whole-cell currents of granule neurons were recorded using a conventional patch-clamp technique. In 6–8 DIC cerebellar GCs, transient I_{Na} are largely unclamped because of an event generated at a site electrotonically distant from the soma and prone to escape from clamp control, presumably the axon [29]. Therefore, we chose those cells that were relatively isolated and only recorded currents without unclamped spike. Prior to current recordings, the culture medium was replaced with a bath solution containing (in mM) NaCl 145, KCl 2.5, HEPES 10, MgCl_2 1 and glucose 10 (pH adjusted to 7.4 using NaOH). Soft glass recording pipettes were filled with an internal solution containing (in mM) CsCl 145, HEPES 10, MgCl_2 2 and EGTA 5 (pH adjusted to 7.3 using CsOH). The pipette resistance was 5–6 $\text{M}\Omega$ after being filled with the internal solution. Whole-cell series resistances of 6–8 $\text{M}\Omega$ were routinely compensated by more than 70%. All currents were recorded using an Axopatch 200B amplifier (Axon Instruments, Foster City, CA, USA) that was operated in voltage-clamp mode. A Pentium computer

was connected to the recording equipment with a Digidata 1300 analogue-to-digital (A/D) interface. The current was digitally sampled at 100 μ s (10 kHz), and the current signals were filtered using a 5-kHz, five-pole Bessel filter. The currents were corrected online for leak and residual capacitance transients using a P/4 protocol. Data acquisition and analysis were performed with pClamp10 software (Axon Instruments) and/or Origin8.1 (MicroCal, Northampton, MA, USA). All recordings were performed at room temperature (23–25°C).

Phosphorylated protein kinase A assay

The cells were lysed in HEPES-NP40 lysis buffer (20 mM HEPES, 150 mM NaCl, 0.5% NP-40, 10% glycerol, 2 mM EDTA, 100 μ M Na₃VO₄, 50 mM NaF and 1% proteinase inhibitor cocktail at pH 7.5) on ice for 30 min. After centrifugation, the supernatant was mixed with 2 \times sodium dodecyl sulphate loading buffer and boiled for 5 min. The proteins were separated on a 10% polyacrylamide gel, transferred to polyvinylidene difluoride membranes (Millipore, Billerica, MA, USA), blocked with 10% non-fat milk and incubated at 4°C overnight with a rabbit polyclonal antibody against the phosphorylated form of the PKA catalytic subunits (1:1000; Santa Cruz Biotechnology Inc., Santa Cruz, CA, USA) or a rabbit monoclonal antibody against GAPDH (1:1000; KangCheng, China). After extensive washing with TBST, the membrane was incubated with horseradish peroxidase-conjugated antimouse or anti-rabbit IgG (1:10,000; KangChen Bio-Tech, Shanghai, China) for 2 hrs at room temperature. Chemiluminescent signals were generated using a SuperSignal West Pico trial kit (Pierce, Rockford, IL, USA) and detected using a ChemiDoc XRS System (Bio-Rad Laboratories Inc., Hercules, CA, USA). The protein measurements were normalized with GAPDH and control/GAPDH as 1.0.

Measurement of intracellular Ca²⁺ levels

Intracellular Ca²⁺ levels were detected by single cell fura-2 AM fluorescence intensity as described by Grynkiewicz [30]. Briefly, cultured cerebellar GCs were rinsed twice with balanced salt solution (BSS), then incubated at 37°C for 45 min. in the presence of 5 μ M fura-2 AM (0.1% dimethylsulfoxide (DMSO) in BSS), washed twice again with BSS and incubated for an additional 20 min. prior to imaging. The BSS was composed of (in mM) NaCl 145, KCl 2.5, HEPES 10, MgCl₂ 1, glucose 10, CaCl₂ 2. The coverslips were transferred to a coverslip chamber, which was mounted on the stage of an inverted phase contrast microscope (Nikon, Eclipse Ti, Japan). Fresh BSS was added to the chamber, and the data were collected at 4-sec. intervals throughout the experiment. The excitation wavelengths for fura-2 AM were 340 and 380 nm, with emission at 505 nm. Baseline [Ca²⁺]_i was determined for 60 sec. immediately prior to the addition of high K⁺ solution (27 mM KCl). Quantification of the fluorescence intensity was performed with Metafluor or software (Universal Imaging Corporation, Downingtown, PA, USA).

Statistical analysis

Statistical analysis was performed with Student's *t*-test with non-paired or paired comparisons, as relevant. The values are given as the means \pm SEM, with *n* representing the number of cells tested. A value of *P* < 0.05 was considered a significant difference between groups.

When multiple comparisons were made, the data were analysed by one-way ANOVA followed by the Tukey and Fisher LSD test for samples of more than two using Originpro software (OriginLab Corporation, Northampton, MA, USA).

Results

First, we investigated the effect of MT on the influence of ELF-EMF on the *I*_{Na} of cerebellar GCs. An *I*_{Na} was elicited by a depolarization step to -20 mV from the holding potential of -100 mV. Our previous study demonstrated that the increase in *I*_{Na} amplitude induced by ELF-EMF exposure was time dependent, and when cerebellar GCs were exposed to 1 mT ELF-EMF for 60 min., the amplitude of the *I*_{Na} increased significantly and was stable [10]. Moreover, exposure cell or neuron to 1–5 mT EMF with short time was reported by Bai and

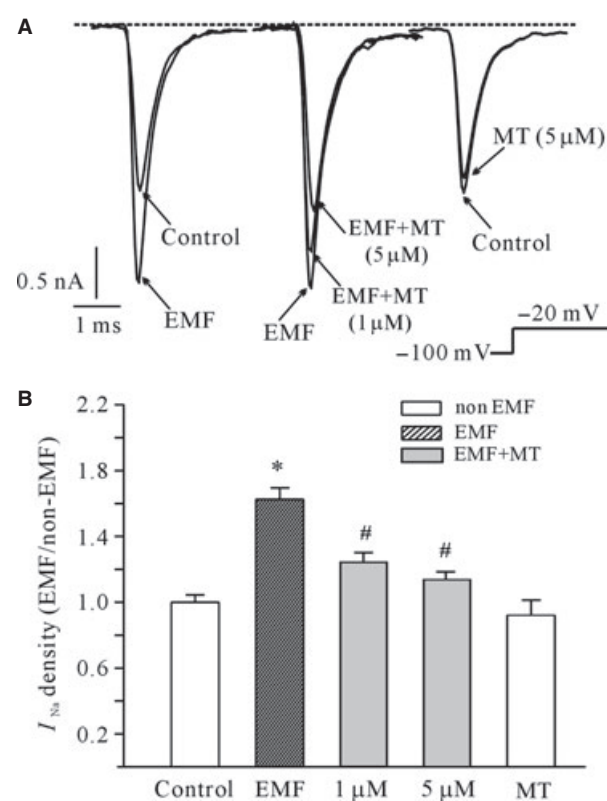


Fig. 1 The effects of melatonin (MT) on increased *I*_{Na} densities induced by exposure to extremely low-frequency electromagnetic field (ELF-EMF). **(A)** Superimposed *I*_{Na} evoked by a 20-msec. depolarizing pulse from a holding potential 100 to -20 mV. Current traces were obtained from cerebellar granule cells exposed to 1 mT ELF-EMF for 60 min. in the presence or absence of MT (1 and 5 μ M). **(B)** Statistical analysis of the effects of MT on increased *I*_{Na} densities induced by exposure to ELF-EMF. The data are reported as the means \pm SEM from 16 to 25 cells. **P* < 0.05 compared with control (non-ELF-EMF) using Student's *t*-test. #*P* < 0.05 compared with the corresponding ELF-EMF control (without MT) using Student's *t*-test.

Moghadam's studies [31, 32]. Therefore, we chose the same parameters of 1 mT ELF-EMF for 60 min. in this study. Similar to our previous report [10], when cerebellar GCs were exposed to 1 mT ELF-EMF for 60 min., the amplitude of the I_{Na} increased by $-62.5 \pm 6.6\%$ ($n = 25$, $P < 0.05$) compared with cells that were not exposed to ELF-EMF ($n = 33$, Fig. 1A). Melatonin significantly inhibited the increase in I_{Na} induced by ELF-EMF. In the presence of 1 μ M or 5 μ M MT, 60 min. of ELF-EMF exposure only increased the I_{Na} by $22.0 \pm 5.9\%$ and $8.9 \pm 4.4\%$ ($n = 15$ and 16 , $P < 0.05$), respectively, which is significantly different from 60 min. of ELF-EMF exposure alone. However, MT alone did not modify I_{Na} activity. There was no significant difference from the control group when 5 μ M MT was added to the bath solution (Fig. 1B).

The inhibitory effect of MT on the ELF-EMF-induced I_{Na} activity could be mimicked by the MT_2 receptor agonist, IIK-7 (Fig. 2A). Similar to MT, IIK7 alone did not affect I_{Na} activity. In the presence of 10 μ M IIK7, the increase in I_{Na} induced by ELF-EMF exposure was reduced from $46.8 \pm 3.5\%$ ($n = 20$) to $-9.2 \pm 6.5\%$ ($n = 27$). This indicates that when IIK7 was used, the I_{Na} densities obtained from exposed cerebellar GCs were reduced by $9.2 \pm 6.5\%$ compared with that of non-ELF-EMF exposure group. Blocking MT_2 with 4-P-PDOT eliminated the inhibitory effect of MT on ELF-EMF-induced I_{Na} activity.

Pre-incubation of cerebellar GCs with 4-P-PDOT (10 μ M) in the medium resulted in an increase in the I_{Na} amplitude after exposure to ELF-EMF by $56.3 \pm 3.0\%$ ($n = 24$). These data were significantly different from that obtained from cells exposed to ELF-EMF with MT ($n = 25$, Fig. 2A). However, 4-P-PDOT (10 μ M) itself did not modify the I_{Na} amplitude (Fig. 2B).

Our previous data indicated that ELF-EMF exposure significantly shifted the voltage dependence of the steady-state activation curve of I_{Na} , but the steady-state inactivation curve of I_{Na} did not significantly shift upon exposure to ELF-EMF [10]. We further investigated whether the inhibitory effects of MT on ELF-EMF-induced I_{Na} activity were because of modulation of the voltage-gating properties of I_{Na} channels. The activation properties of I_{Na} in cerebellar GCs following exposure to ELF-EMF were studied using the appropriate voltage protocols. I_{Na} was evoked by a 20-msec. depolarizing pulse from a holding potential of -100 mV to potentials between -70 and 20 mV, with 5-mV steps in 5-sec. intervals (Fig. 3A). A value for the steady-state activation of I_{Na} was then obtained by normalizing the conductance as a function of the command potential; conductance was calculated as $G_{Na} = I_{Na}/(V_{m1/2} - V_{rev})$. The data points were fitted to the Boltzmann function $G_{Na}/G_{Na-max} = 1/\{1+\exp [(V_{m1/2} - V_m)/k]\}$, and the half-activation potentials were calculated. Figure 3B illustrates the steady-state activa-

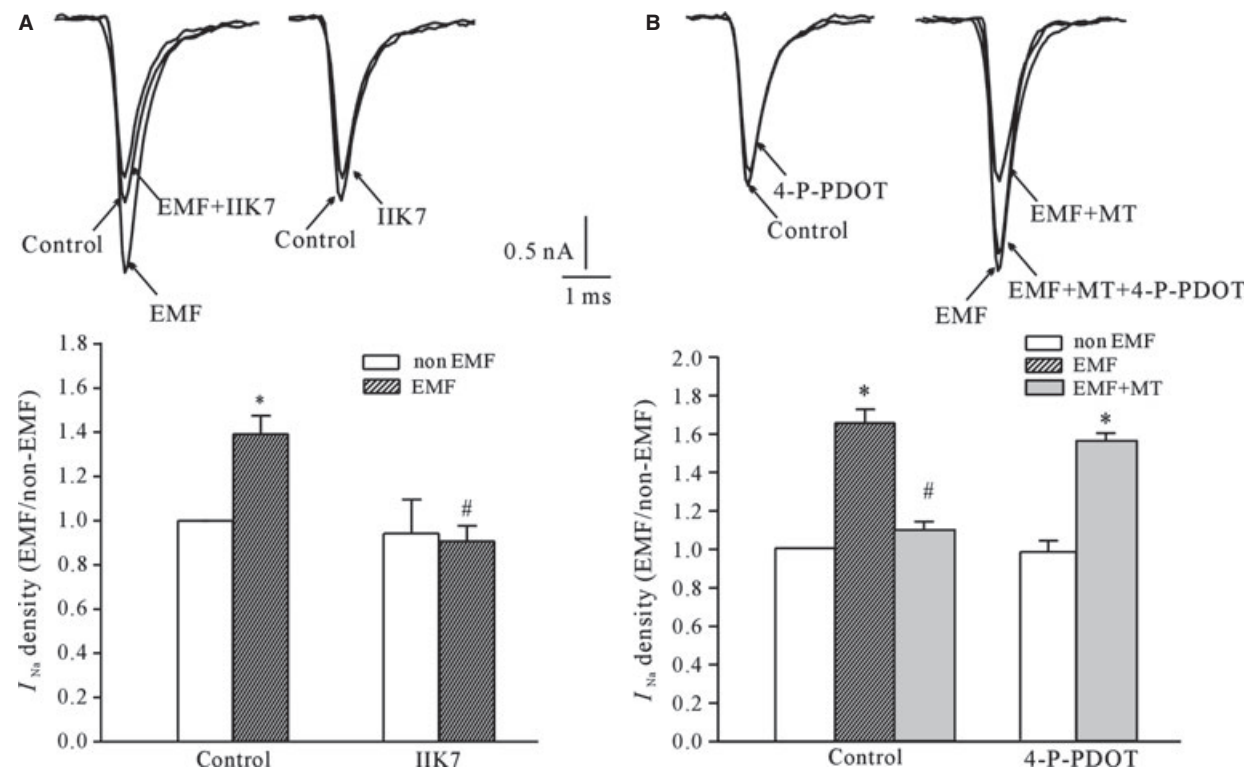


Fig. 2 The effects of MT_2 receptor agonist and antagonist on the melatonin (MT)-mediated inhibitory effects on extremely low-frequency electromagnetic field (ELF-EMF) exposure-induced I_{Na} enhancement. **(A)** Current traces and statistical analysis show the effects of the selective MT_2 R agonist IIK7 on I_{Na} obtained from ELF-EMF- and non-ELF-EMF-exposed groups. **(B)** Current traces and statistical analysis show the effects of the selective MT_2 R antagonist 4-P-PDOT on MT-induced inhibition of I_{Na} in ELF-EMF-exposed cerebellar granule cells. * $P < 0.05$ compared with the corresponding control (non-ELF-EMF exposed) using Student's t -test. # $P < 0.05$ compared with ELF-EMF exposed without MT using Student's t -test.

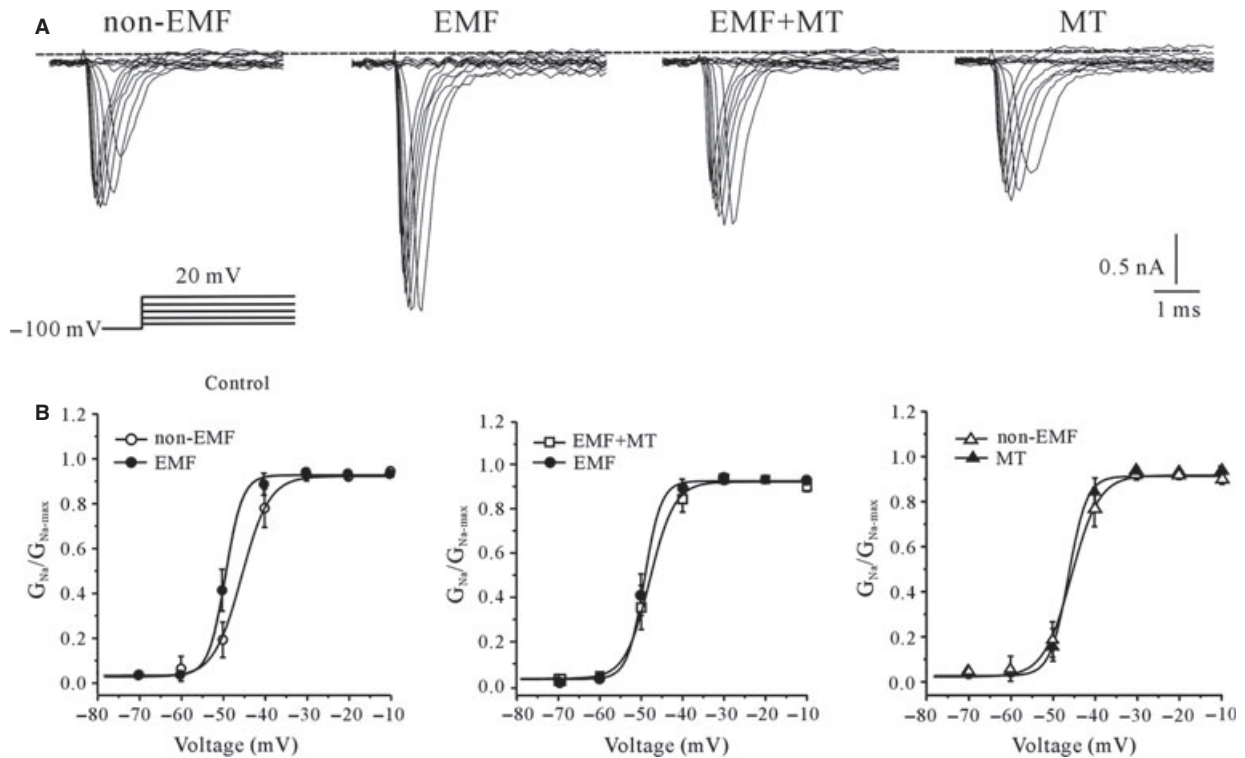


Fig. 3 The effect of melatonin (MT) on the steady-state activation property of I_{Na} channels in extremely low-frequency electromagnetic field (ELF-EMF)-exposed and non-ELF-EMF-exposed cerebellar granule cells (GCs). **(A)** Representative superimposed I_{Na} evoked by steady-state activation voltage protocol obtained from non-ELF-EMF- and ELF-EMF-exposed cerebellar GCs in the presence and absence of MT. The cells were held at -100 mV and depolarized in 5-mV steps from -70 to 20 mV with intervals of 5 sec. **(B)** The voltage-dependent activation curve of I_{Na} obtained from non-ELF-EMF- and ELF-EMF-exposed cerebellar GCs in the presence and absence of MT. The data are expressed as the means \pm SEM from 13 to 12 cells.

tion curve of I_{Na} obtained from cerebellar GCs that were exposed to ELF-EMF with or without MT. The half-activation potentials obtained from the control GC group was -43.3 ± 2.1 mV, which shifted to -48.8 ± 1.3 mV ($n = 14$, $P < 0.05$) when cerebellar GCs were exposed to ELF-EMF. In the presence of MT, the half-activation potentials were -44.2 ± 1.1 mV for GCs with no ELF-EMF exposure ($n = 6$) and -47.7 ± 1.7 mV for GCs exposed to ELF-EMF ($n = 12$). These data suggest that MT did not modify the steady-state activation property of the I_{Na} channels of the cerebellar GCs regardless of whether they were exposed to ELF-EMF.

Our previous study showed that the I_{Na} of cerebellar GCs was enhanced by activation of PKA [33], and a significant increase in the intracellular levels of phosphorylated PKA (pPKA), as measured using an immunoblot assay, was observed following ELF-EMF exposure [10]. We thus studied the effect of MT on intracellular pPKA levels to address whether MT functioned by inhibiting the PKA activity. Unexpectedly, both MT and IIK-7 increased the intracellular pPKA by $15.1 \pm 5.0\%$ and $16.2 \pm 7.3\%$ respectively ($n = 8$, $P < 0.05$; Fig. 4A and B). The presence of MT or IIK-7 did not inhibit the ELF-EMF exposure-induced increase in intracellular pPKA (Fig. 4A and B), which was $26.3 \pm 8.7\%$ for MT and $29.4 \pm 7.3\%$ for IIK-7 ($n = 8$,

$P < 0.05$). These results suggest that PKA activation is not associated with the inhibitory effect of MT on the ELF-EMF exposure-induced increase in I_{Na} channel activity.

It has previously been reported that Ca^{2+}/CaM can modulate voltage-gated Na^+ channels in neurons and muscles [34, 35]. We therefore examined the effects of KN-93, a $Ca^{2+}/CaMKII$ blocker, on the inhibitory effect of MT on the ELF-EMF exposure-induced increase in I_{Na} channel activity. KN-93 alone did not modify the I_{Na} amplitude. In the presence of KN-93 ($10 \mu M$), the I_{Na} amplitude after ELF-EMF exposure with MT was increased from $8.9 \pm 4.4\%$ to $49.4 \pm 17.1\%$ ($n = 19$; Fig. 5A), which was significantly different from the results obtained without KN-93 ($P < 0.05$), suggesting that the Ca^{2+}/CaM pathway is associated with the inhibitory effect of MT on the ELF-EMF exposure-induced increase in I_{Na} . We then tested the effect on ELF-EMF exposure-induced increase in I_{Na} by treatment of C_6 -ceramide, which increases Ca^{2+} release through the ryanodine-sensitive Ca^{2+} receptor [35]. Based on our results, C_6 -ceramide could mimic the effect of MT and decreased the ELF-EMF-induced inhibitory effect in I_{Na} from $71.2 \pm 8.0\%$ to $16.8 \pm 11.7\%$ ($n = 11$, Fig. 5B). In rat cerebellar GCs, intracellular Ca^{2+} is mainly released by the ryanodine-sensitive Ca^{2+} receptor pathway [35]. Therefore, we used ruthenium

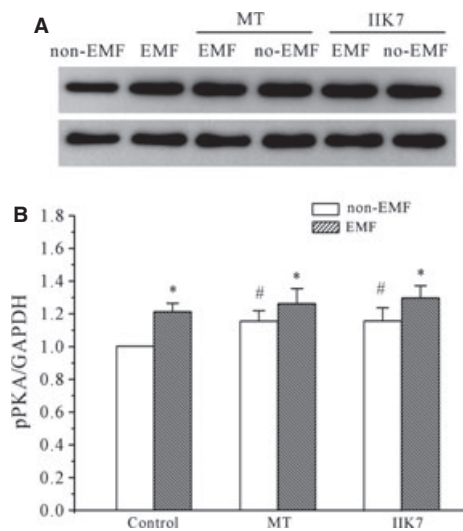


Fig. 4 The effect of melatonin (MT) and IIK-7 on the PKA activity in extremely low-frequency electromagnetic field (ELF-EMF)- and non-ELF-EMF-exposed cerebellar granule cells (GCs) measured by Western blot analysis. **(A)** Representative samples show the effects of MT and IIK-7 on PKA levels. **(B)** The statistical analysis of the effects of MT and IIK-7 on PKA levels in ELF-EMF- and non-ELF-EMF-exposed cerebellar GCs. * $P < 0.05$ compared with non-ELF-EMF-exposed controls using Student's t -test. # $P < 0.05$ compared with the corresponding non-ELF-EMF-exposed control without MT or IIK-7 using Student's t -test.

red, a ryanodine-sensitive receptor blocker, to probe whether the inhibitory effect of MT on the ELF-EMF exposure-induced increase in I_{Na} is through ryanodine-sensitive Ca^{2+} receptor-induced calcium release. Consistent with previous reports by Claire O. Malecot *et al.* [36], incubation of rat cerebellar GCs with ruthenium red (10 μ M) alone significantly reduced I_{Na} amplitude. On the other hand, blocking ryanodine-sensitive Ca^{2+} receptor by ruthenium red significantly eliminated the inhibitory effect of MT on the ELF-EMF exposure-induced increase in I_{Na} : in the presence of ruthenium red (10 μ M), the I_{Na} amplitude after ELF-EMF exposure with MT was still increased $85.4 \pm 8.1\%$ ($n = 9$) compared with the group treated with ruthenium red alone (Fig. 5C).

To confirm that intracellular Ca^{2+} was associated with the inhibitory effect of MT on ELF-EMF-induced I_{Na} activity, we used direct Ca^{2+} imaging using the calcium-sensitive fluorescent dye fura-2 AM to examine the potential effects of MT on intracellular calcium levels in cerebellar GCs. Because MT did not affect the basal level of intracellular calcium of cerebellar GCs, we used a high K^+ -solution (27 mM KCl) to depolarize neurons and activate voltage-dependent Ca^{2+} channels (VGCCs), leading to a rapid increase in the calcium concentration [37]. In control neurons, depolarization stimulation by high K^+ evoked an acute elevation of intracellular Ca^{2+} levels with an increase in the F340/F380 ratio from 0.37 ± 0.006 to 1.25 ± 0.061 ($n = 26$), depicting as a shift from purple to red. After exposure to ELF-EMF, the high K^+ stimulation evoked a similar intracellular Ca^{2+} level increase from 0.35 ± 0.016 to 1.21 ± 0.055 ($n = 25$), which

was not significantly different compared with the group with non-ELF-EMF exposure (Fig. 6A and B). Melatonin did not increase the basal intracellular Ca^{2+} level, but it significantly elevated the intracellular Ca^{2+} level evoked by high K^+ stimulation in cerebellar GCs that were either exposed to ELF-EMF or not (Fig. 6A and B). In the presence of MT, the intracellular Ca^{2+} F340/F380 ratio evoked by high K^+ stimulation was significantly increased in cerebellar GCs that were either exposed to ELF-EMF or not to 1.62 ± 0.064 ($n = 35$) and 1.52 ± 0.055 ($n = 31$), respectively (Fig. 6B), which was significantly different from the 1.21 ± 0.055 and 1.25 ± 0.061 recorded in the absence of MT. Increases in intracellular Ca^{2+} levels were calculated as a percentage of the control based on the F340/F380 ratio and were $29.6 \pm 11.0\%$ and $21.2 \pm 9.6\%$, respectively, (Fig. 6C) for cerebellar GCs that were either exposed to ELF-EMF or not. However, when Ca^{2+} was removed from bath solution, depolarization stimulation by high K^+ did not increase the intracellular Ca^{2+} levels, suggesting that extracellular Ca^{2+} influx was needed for the depolarization-induced intracellular Ca^{2+} increase (Fig. 6A–C).

We also used ruthenium red to address whether the MT-induced increase in calcium release occurred through the ryanodine-sensitive Ca^{2+} receptor. Pre-incubation of cerebellar GCs with 20 μ M ruthenium red alone induced a slight reduction in the F340/F380 ratio stimulated by high K^+ from 1.25 ± 0.061 to 0.91 ± 0.050 ($n = 28$; Fig. 7A and B), which was an inhibition of $19.2 \pm 8.8\%$ compared with the control group (Fig. 7C); in the presence of ruthenium red, the increase in the F340/F380 ratio induced by MT was reduced from 1.52 ± 0.055 to 1.01 ± 0.037 ($n = 24$) in the control group. Similarly, ruthenium red also significantly inhibited the effect of MT on intracellular Ca^{2+} release after ELF-EMF exposure, which resulted in a decrease in the F340/F380 ratio from 1.62 ± 0.064 to 1.07 ± 0.078 ($n = 34$; Fig. 7C).

Discussion

Although several ion channels, such as delayed rectifier outward K^+ current (I_K), TRPM-2 and voltage-dependent L-type Ca^{2+} channels, are known to be modulated by MT [18–21], the effects of MT on Na_v channels are poorly understood. Although MT has previously been reported to protect cells against EMF stimulus, whether it modulates the activity of ion channels induced by EMF exposure is poorly understood. Here, we report for the first time that MT itself was not able to modify I_{Na} , but might inhibit I_{Na} enhancement resulting from ELF-EMF exposure in cerebellar GCs by increasing the concentration of intracellular Ca^{2+} .

It is well known that the effects of exposure to EMF differ significantly based on the ELF-EMF exposure intensities and the exposure time. Our previous study indicates that exposure of cerebellar GCs to ELF-EMF (1 mT) for short time (10–60 min.) significantly increases the amplitude of the I_{Na} . Moreover, exposure to ELF-EMF induces similar effects on I_{Na} in rat cerebellar GCs regardless the condition, whether it is 1 mT stimulation for a short time or 0.4 mT stimulation for a longer time. Notably, it is generally believed that short-term changes induced by EMF are mediated by modifications in enzyme activity in the cytosol or the membrane [4, 38, 39], while the long-

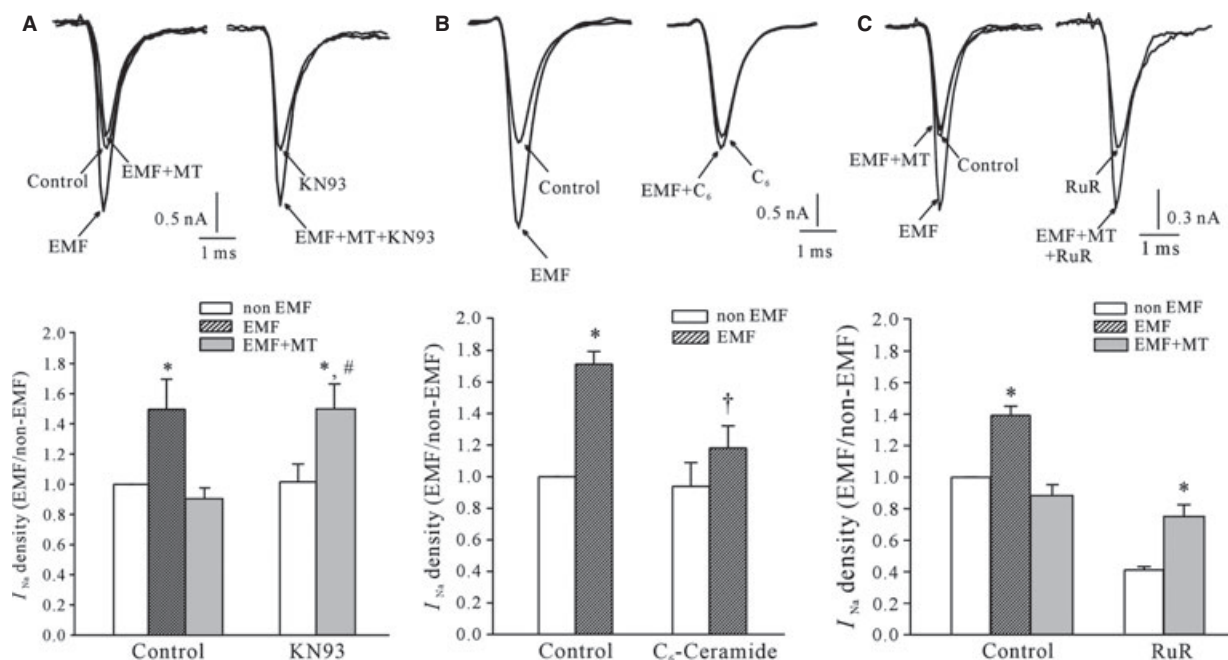


Fig. 5 Current traces and statistical analysis show the effects of the $\text{Ca}^{2+}/\text{CaM}$ pathway on melatonin (MT)-induced inhibition of I_{Na} in extremely low-frequency electromagnetic field (ELF-EMF)-exposed cerebellar granule cells. **(A)** Representative superimposed I_{Na} traces and statistical analysis showing that KN-93 significantly abolished the effect of MT on the EMF-induced I_{Na} increase. **(B)** Representative superimposed I_{Na} traces and statistical analysis showed that C_6 -ceramide (C_6) could mimic the effect of MT on the EMF-induced I_{Na} increase. **(C)** Representative superimposed I_{Na} traces and statistical analysis showed that ruthenium red (RuR) significantly abolished the effect of MT on the EMF-induced I_{Na} increase. * $P < 0.05$ compared with the non-ELF-EMF-exposed controls using Student's t -test. # $P < 0.05$ compared with the corresponding control (ELF-EMF exposed to MT) using Student's t -test. † $P < 0.05$ compared with the corresponding control without C_6 -ceramide treatment using Student's t -test.

term exposure to EMF may induce changes in nuclear functions such as gene transcription and cell cycle regulation [27, 40]. To avoid the influence of multiple factors because of long-term EMF exposure, we performed all our experiments at 1 mT EMF exposure for a short time, which we believe that it is suitable to assess the effect of ELF-EMF on intracellular signalling pathways.

Although some of the main functions attributed to MT include its role as a free radical scavenger and its indirect antioxidant properties [41], studies have shown that MT can interact with specific receptors to exert its biological effect [42]. Our previous study demonstrated that activation of the MT_2 receptor (MT_2R) by MT and a low concentration of 2-iodomelatonin increased the delayed-rectified outward K^+ current (I_{K}) [43] and improved cerebellar GC migration [21]. In contrast, a high concentration of 2-iodomelatonin could inhibit the I_{K} recorded from cerebellar GCs by activating the MT_1 receptor, which protects the neurons against apoptotic stimulus [20]. In this study, a selective MT_2 agonist could mimic the effect of MT on EMF-induced I_{Na} enhancement, which could be blocked by a selective MT_2 antagonist, suggesting that it is highly likely that the inhibitory effect of MT on EMF-induced I_{Na} enhancement was mediated by MT_2R , and did not directly result from the antioxidant properties of MT. This is consistent with our previous findings on the effect of MT on the potassium current in cerebellar GCs [20, 21, 43].

Among the possible mechanisms underlying the inhibitory effect of MT on EMF-induced I_{Na} increase, we first considered the involvement of the MT_2 -mediated cAMP/PKA pathway because EMF-induced I_{Na} increase is thought to occur via the cAMP/PKA pathway [10], and negative modulation of cAMP/PKA activation by MT has previously been reported [21]. However, the experimental data presented here show that MT did not inhibit PKA activity; instead, it induced a slight increase in PKA activity. Furthermore, MT was not able to inhibit the PKA activity induced by EMF exposure. In addition, MT did not change the steady-state activity of I_{Na} channels in the control cerebellar GCs or in EMF-exposed cerebellar GCs, indicating that a non-phosphorylation-dependent mechanism is involved. Together, these data suggest that the ability of MT to counteract the effect of EMF on I_{Na} activity does not occur through the inhibition of EMF-induced PKA activity. MT failed to negatively modulate PKA activity in this study, which is different from what has previously been reported [21]. This effect might be as a result of the higher concentration of MT used in this study. Transfection experiments have demonstrated that when expressed in the same cell type, MT_1 and MT_2 receptors may couple to different signalling pathways [44]. Both our work and that of Marta indicate that the presence of native MT_1/MT_2 receptors in mouse and rat cerebellar GCs mediates the effects of MT on intracellular signalling pathways [20, 21, 45]. Thus, it is possible that 1–5 μM MT may

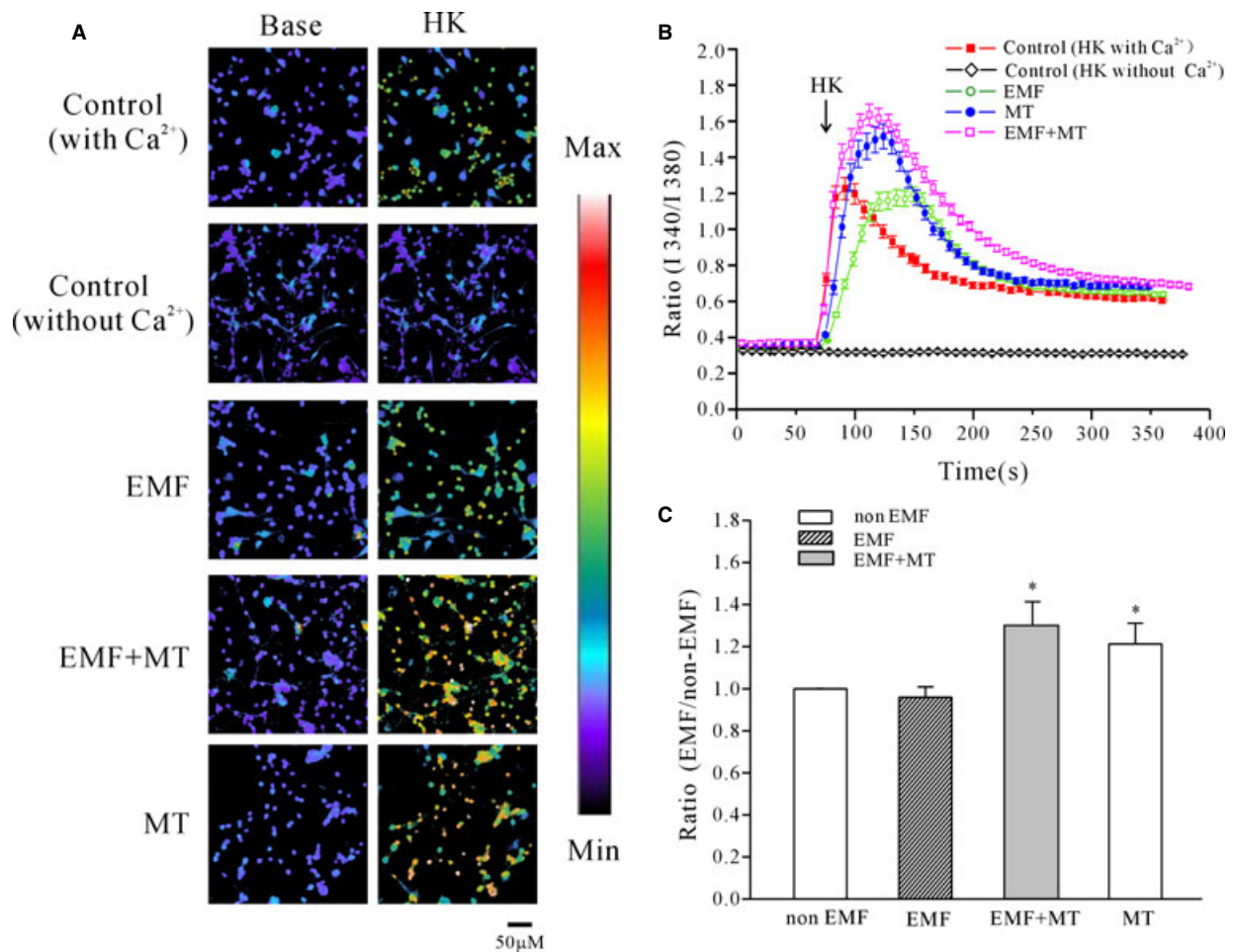


Fig. 6 Effect of melatonin (MT) on the increase in intracellular Ca^{2+} level induced by high K^+ in control cells and cells exposed to extremely low-frequency electromagnetic field (ELF-EMF). (A) $[\text{Ca}^{2+}]_i$ imaging obtained before and after depolarizing membranes by acute perfusion of a solution containing 27 mM K^+ from ELF-EMF exposure and control cerebellar granule cells (GCs) in the presence or absence of MT. Changes in the fura-2 AM fluorescence excitation ratios with increasing $[\text{Ca}^{2+}]_i$ are depicted as a switch from purple to red; scale bar, 50 μm . (B) Changes in intracellular Ca^{2+} concentrations upon application of a depolarizing stimulus as measured by quantification of fluorescence excitation ratios. Each arrow represents a 30-sec. perfusion with a depolarizing solution containing 27 mM K^+ . (C) Statistical analysis of intracellular Ca^{2+} level obtained from ELF-EMF-exposed and control cerebellar GCs in the presence or absence of MT. The data were obtained from four independent experiments and are the means \pm SEM; * $P < 0.05$ compared with the corresponding control by unpaired t -test.

activate both MT_1 and MT_2 receptors simultaneously, thereby inducing a coordinated and integrated effect on PKA. Therefore, the effect of MT on the PKA pathway was no longer evident.

In addition to the cAMP/PKA pathway, Ca^{2+} has been proposed to regulate Na^+ channels through the action of calmodulin (CaM) bound to an isoleucine–glutamine motif in the C terminus of the Na^+ channel subunit [46]. Previous studies indicate that MT modulates the Ca^{2+} /CaM signalling pathway either by changing the intracellular calcium concentration ($[\text{Ca}^{2+}]_i$) via activation of its G-protein coupled membrane receptors or through a direct interaction with CaM [47, 48]. MT was shown to be able to reverse cytosolic Ca^{2+} evoked by H_2O_2 stimuli [19]. In rat cerebellar GCs, intracellular Ca^{2+} is mainly released by

the ryanodine-sensitive Ca^{2+} receptor pathway, which might maintain I_{Na} at a lower level [34]. In this study, the Ca^{2+} /CaMKII and ryanodine-sensitive Ca^{2+} receptor blocker significantly abolished the effect of MT on the EMF-induced I_{Na} increase, providing evidence for the involvement of the Ca^{2+} /CaM pathway. Interestingly, MT did not increase basal Ca^{2+} release, but significantly increased high K^+ evoked intracellular Ca^{2+} levels, which was thought to result from membrane depolarization [49]. Furthermore, the increase in intracellular Ca^{2+} evoked by MT was inhibited when the ryanodine-sensitive Ca^{2+} receptor was blocked with ruthenium red. It is thus highly likely that MT activated the MT_2R -mediated Ca^{2+} channels and improved extracellular Ca^{2+} influx, which consequently stimulated the release of Ca^{2+}

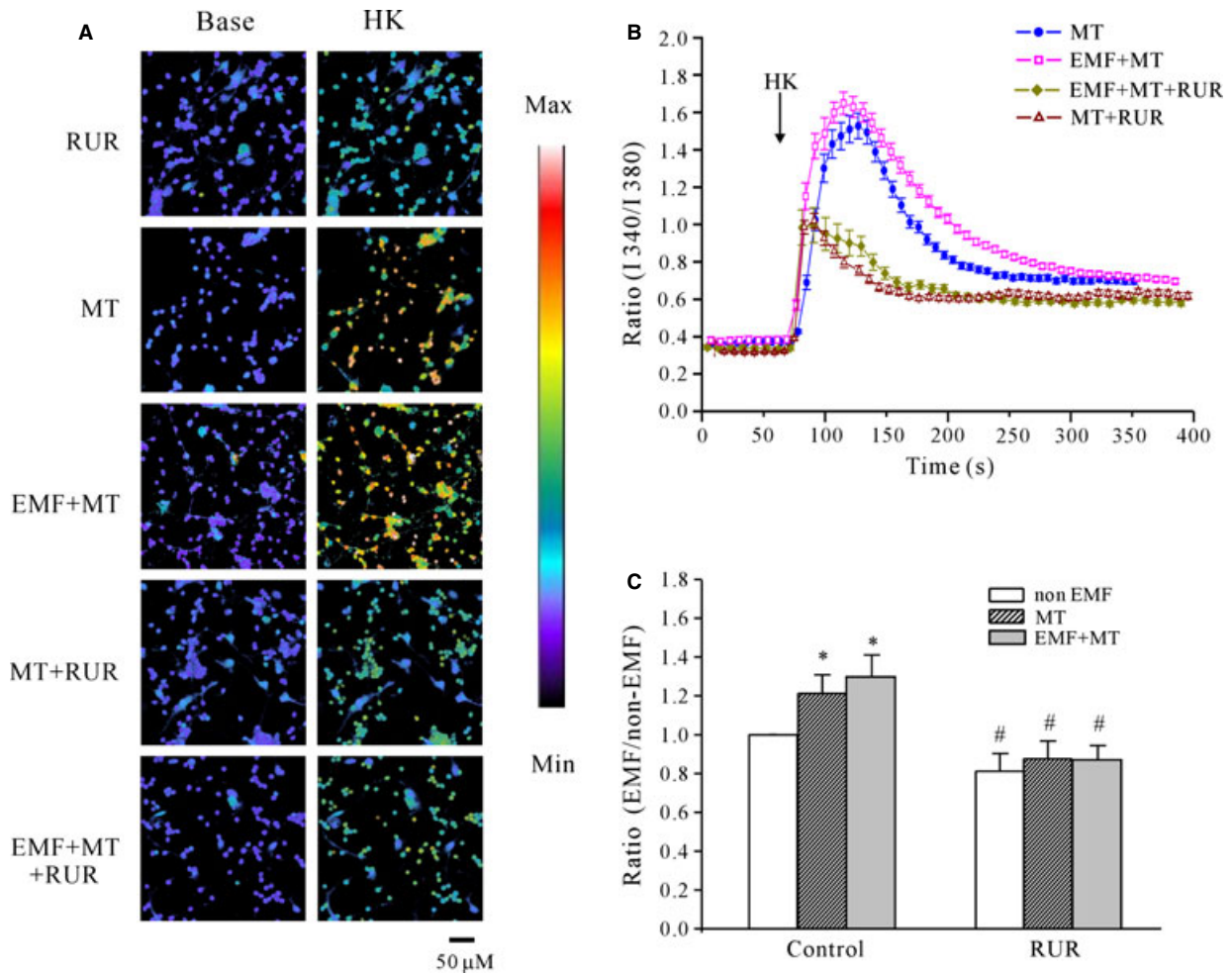


Fig. 7 Effects of blocking ryanodine-sensitive receptors on melatonin (MT)-induced increase in intracellular Ca^{2+} level in control cells and cells exposed to extremely low-frequency electromagnetic field (ELF-EMF). **(A)** $[\text{Ca}^{2+}]$ imaging obtained before and after depolarizing membranes by acute perfusion of a solution containing 27 mM K^+ from ELF-EMF-exposed cells with MT in the presence or absence of Ruthenium Red (RuR, 20 μM); scale bar, 50 μm . **(B)** Changes in intracellular calcium concentrations upon application of RuR. Each arrow represents a 30-sec. perfusion with a depolarizing solution containing 27 mM K^+ . **(C)** Statistical analysis of intracellular Ca^{2+} levels obtained after ELF-EMF exposure with MT in the presence or absence of RuR. The data are the means \pm SEM obtained from four independent experiments; * $P < 0.05$ compared with non-ELF-EMF-exposed cells without MT using Student's t -test. # $P < 0.05$ compared with the corresponding control by unpaired t -test.

through the ryanodine-sensitive Ca^{2+} receptor, by which the EMF-induced I_{Na} increase was reversed.

However, our previous study with Western blotting has revealed [10] that ELF-EML increases the current density by increasing the Na_v channel protein expression on cerebellar GCs membrane, although the content of expression is lower. Whether increase in Na_v channel protein expression or else mechanism is involved in MT-induced and Ca^{2+} /CaM-dependent modulation of I_{Na} amplitude remains unclear, and further study is necessary.

Taken together, our data suggest that MT eliminated the EMF-induced I_{Na} increase through Ca^{2+} influx-induced Ca^{2+} release but not by abolishing EMF-induced PKA activity. However, we noticed

that MT itself did not affect the amplitude of I_{Na} in control cerebellar GCs, although it was able to increase the intracellular Ca^{2+} levels evoked by high K^+ depolarization stimuli. This might be because basal intracellular Ca^{2+} released from ryanodine-sensitive receptors maintain the I_{Na} at a low enough level in rat cerebellar GCs [34] that MT-induced Ca^{2+} release is not able to reduce the I_{Na} densities further. However, when cerebellar GCs were exposed to EMF with MT, high K^+ -mediated Ca^{2+} release was significantly enhanced, and MT reversed the EMF-induced increase in I_{Na} amplitude. This observation was consistent with previous studies that indicated that most of the effects of MT on second messengers or effectors require prior stimulatory input [50, 51]. It is highly likely

that with EMF exposure as stimulatory input, the effect of MT on I_{Na} could be fully realized.

Currently, there is widespread use of EMR-emitting devices in industrial, scientific, medical and domestic applications, with the potential for leakage of such radiation into the environment [52]. The effects of ELF-EMF on nerve cells have been extensively studied in various organisms [8, 53]. Although the reported results are variable or contradictory because of differences in the experimental conditions and in the density and/or duration of EMF exposure, EMF has recently been reported to modulate neuronal excitatory functions and neurogenesis [8, 24, 25]. The findings from our molecular-level analysis of the protective effects of MT on I_{Na} produced by exposure to ELF-EMF might provide evidence for an important effect of MT on neuronal excitation during EMF exposure in cerebellar GCs. Nonetheless, the modulatory effects on neuronal excitatory functions caused by exposure to ELF-EMF are complicated and varied. In addition, the functional mechanism of MT and its receptors in native cerebellar GCs are complex. Therefore, further exploration is required to comprehensively analyse the biological protective effects of MT and its mechanism on neurons that are exposed to ELF-EMF.

References

1. Cui Y, Ge Z, Rizak JD, *et al.* Deficits in water maze performance and oxidative stress in the hippocampus and striatum induced by extremely low frequency magnetic field exposure. *PLoS ONE*. 2012; 7: e32196.
2. Luukkonen J, Liimatainen A, Hoyto A, *et al.* Pre-exposure to 50 Hz magnetic fields modifies menadione-induced genotoxic effects in human SH-SY5Y neuroblastoma cells. *PLoS ONE*. 2011; 6: e18021.
3. Piacentini R, Ripoli C, Mezzogori D, *et al.* Extremely low-frequency electromagnetic fields promote *in vitro* neurogenesis via upregulation of Ca(v)1-channel activity. *J Cell Physiol*. 2008; 215: 129–39.
4. Arendash GW, Mori T, Dorsey M, *et al.* Electromagnetic treatment to old Alzheimer's mice reverses beta-amyloid deposition, modifies cerebral blood flow, and provides selected cognitive benefit. *PLoS ONE*. 2012; 7: e35751.
5. Dibirdik I, Kristupaitis D, Kurosaki T, *et al.* Stimulation of Src family protein-tyrosine kinases as a proximal and mandatory step for SYK kinase-dependent phospholipase Cgamma2 activation in lymphoma B cells exposed to low energy electromagnetic fields. *J Biol Chem*. 1998; 273: 4035–9.
6. Sun WJ, Chiang H, Fu YT, *et al.* Exposure to 50 Hz electromagnetic fields induces the phosphorylation and activity of stress-activated protein kinase in cultured cells. *Electro Magnetobiol*. 2001; 20: 415–23.
7. Ramundo-Orlando A, Mattia F, Palombo A, *et al.* Effect of low frequency, low amplitude magnetic fields on the permeability of cationic liposomes entrapping carbonic anhydrase: II. No evidence for surface enzyme involvement. *Bioelectromagnetics*. 2000; 21: 499–507.
8. Marchionni I, Paffi A, Pellegrino M, *et al.* Comparison between low-level 50 Hz and 900 MHz electromagnetic stimulation on single channel ionic currents and on firing frequency in dorsal root ganglion isolated neurons. *Biochim Biophys Acta*. 2006; 1758: 597–605.
9. Pall ML. Electromagnetic fields act *via* activation of voltage-gated calcium channels to produce beneficial or adverse effects. *J Cell Mol Med*. 2013; 17: 958–65.
10. He YL, Liu DD, Fang YJ, *et al.* Exposure to extremely low-frequency electromagnetic fields modulates Na⁺ currents in rat cerebellar granule cells through increase of AA/PGE2 and EP receptor-mediated cAMP/PKA pathway. *PLoS ONE*. 2013; 8: e54376.
11. Hardeland R, Madrid JA, Tan DX, *et al.* Melatonin, the circadian multioscillator system and health: the need for detailed analyses of peripheral melatonin signaling. *J Pineal Res*. 2012; 52: 139–66.
12. Calvo JR, Gonzalez-Yanes C, Maldonado MD. The role of melatonin in the cells of the innate immunity: a review. *J Pineal Res*. 2013; 55: 103–20.
13. Reiter RJ, Tan DX, Manchester LC, *et al.* Biochemical reactivity of melatonin with reactive oxygen and nitrogen species: a review of the evidence. *Cell Biochem Biophys*. 2001; 34: 237–56.
14. Galano A, Tan DX, Reiter RJ. Melatonin as a natural ally against oxidative stress: a physicochemical examination. *J Pineal Res*. 2011; 51: 1–16.
15. Galano A, Tan DX, Reiter RJ. On the free radical scavenging activities of melatonin's metabolites, AFMK and AMK. *J Pineal Res*. 2013; 54: 245–57.
16. Naziroglu M, Tokat S, Demirci S. Role of melatonin on electromagnetic radiation-induced oxidative stress and Ca²⁺ signaling molecular pathways in breast cancer. *J Recept Signal Transduct Res*. 2012; 32: 290–7.
17. Vijayalaxmi, Reiter RJ, Meltz ML, *et al.* Melatonin: possible mechanisms involved in its 'radioprotective' effect. *Mutat Res*. 1998; 404: 187–9.
18. Naziroglu M, Celik O, Ozgul C, *et al.* Melatonin modulates wireless (2.45 GHz)-induced oxidative injury through TRPM2 and voltage gated Ca(2+) channels in brain and dorsal root ganglion in rat. *Physiol Behav*. 2012; 105: 683–92.
19. Celik O, Naziroglu M. Melatonin modulates apoptosis and TRPM2 channels in transfected cells activated by oxidative stress. *Physiol Behav*. 2012; 107: 458–65.

Acknowledgements

The study was supported by a grant from the National Basic Research Program of China (2011CB503703) and the Shanghai Leading Academic Discipline Project (B111). Qian-Ru zhao was supported by the National Talent Training Fund in Basic Research of China (No. J1210012).

Conflicts of interest

The authors confirm that there are no conflicts of interest.

Author contribution

Dong-Dong Liu performed experiments, analysed data, interpreted results of experiments and prepared figures; Zheng Ren helped to perform experiments and analyse data; Guang Yang and Qian-Ru zhao helped to perform experiments, analyse data and interpret results of experiments; Yan-Ai Mei contributed to the design of research, drafted the manuscript and approved the final version of manuscript.

20. **Jiao S, Wu MM, Hu CL, et al.** Melatonin receptor agonist 2-iodomelatonin prevents apoptosis of cerebellar granule neurons via K(+) current inhibition. *J Pineal Res.* 2004; 36: 109–16.
21. **Liu LY, Hoffman GE, Fei XW, et al.** Delayed rectifier outward K⁺ current mediates the migration of rat cerebellar granule cells stimulated by melatonin. *J Neurochem.* 2007; 102: 333–44.
22. **Banasiak KJ, Burenkova O, Haddad GG.** Activation of voltage-sensitive sodium channels during oxygen deprivation leads to apoptotic neuronal death. *Neuroscience.* 2004; 126: 31–44.
23. **Ding Y, Brackenbury WJ, Onganer PU, et al.** Epidermal growth factor upregulates motility of Mat-LyLu rat prostate cancer cells partially via voltage-gated Na⁺ channel activity. *J Cell Physiol.* 2008; 215: 77–81.
24. **Aldinucci C, Carretta A, Maiorca SM, et al.** Effects of 50 Hz electromagnetic fields on rat cortical synaptosomes. *Toxicol Ind Health.* 2009; 25: 249–52.
25. **Cuccurazzu B, Leone L, Podda MV, et al.** Exposure to extremely low-frequency (50 Hz) electromagnetic fields enhances adult hippocampal neurogenesis in C57BL/6 mice. *Exp Neurol.* 2010; 226: 173–82.
26. **Gonzalez B, Leroux P, Lamacz M, et al.** Somatostatin receptors are expressed by immature cerebellar granule cells: evidence for a direct inhibitory effect of somatostatin on neuroblast activity. *Proc Natl Acad Sci USA.* 1992; 89: 9627–31.
27. **Ongaro A, Varani K, Masieri FF, et al.** Electromagnetic fields (EMFs) and adenosine receptors modulate prostaglandin E(2) and cytokine release in human osteoarthritic synovial fibroblasts. *J Cell Physiol.* 2012; 227: 2461–9.
28. **Varani K, Vincenzi F, Targa M, et al.** Effect of pulsed electromagnetic field exposure on adenosine receptors in rat brain. *Bioelectromagnetics.* 2012; 33: 279–87.
29. **Diwakar S, Magistretti J, Goldfarb M, et al.** Axonal Na⁺ channels ensure fast spike activation and back-propagation in cerebellar granule cells. *J Neurophysiol.* 2009; 101: 519–32.
30. **Grynkiewicz G, Poenie M, Tsien RY.** A new generation of Ca²⁺ indicators with greatly improved fluorescence properties. *J Biol Chem.* 1985; 260: 3440–50.
31. **Bai WF, Xu WC, Feng Y, et al.** Fifty-Hertz electromagnetic fields facilitate the induction of rat bone mesenchymal stromal cells to differentiate into functional neurons. *Cytotherapy.* 2013; 15: 961–70.
32. **Moghadam MK, Firoozabadi M, Janahmadi M.** Effects of weak environmental magnetic fields on the spontaneous bioelectrical activity of snail neurons. *J Membr Biol.* 2011; 240: 63–71.
33. **Fang YJ, Zhou MH, Gao XF, et al.** Arachidonic acid modulates Na⁺ currents by non-metabolic and metabolic pathways in rat cerebellar granule cells. *Biochem J.* 2011; 438: 203–15.
34. **Liu Z, Xu JG, Zhang H, et al.** C(6)-ceramide inhibited Na⁽⁺⁾ currents by intracellular Ca (2+) release in rat myoblasts. *J Cell Physiol.* 2007; 213: 151–60.
35. **Liu Z, Fei XW, Fang YJ, et al.** PLC-dependent intracellular Ca²⁺ release was associated with C6-ceramide-induced inhibition of Na⁺ current in rat granule cells. *J Neurochem.* 2008; 106: 2463–75.
36. **Malecot CO, Bito V, Argibay JA.** Ruthenium red as an effective blocker of calcium and sodium currents in guinea-pig isolated ventricular heart cells. *Br J Pharmacol.* 1998; 124: 465–72.
37. **Gutierrez-Martin Y, Martin-Romero FJ, Henao F, et al.** Alteration of cytosolic free calcium homeostasis by SIN-1: high sensitivity of L-type Ca²⁺ channels to extracellular oxidative/nitrosative stress in cerebellar granule cells. *J Neurochem.* 2005; 92: 973–89.
38. **Morelli A, Ravera S, Panfoli I, et al.** Effects of extremely low frequency electromagnetic fields on membrane-associated enzymes. *Arch Biochem Biophys.* 2005; 441: 191–8.
39. **Ravera S, Bianco B, Cugnoli C, et al.** Sinusoidal ELF magnetic fields affect acetylcholinesterase activity in cerebellum synaptosomal membranes. *Bioelectromagnetics.* 2010; 31: 270–6.
40. **Richard D, Lange S, Vieregutz T, et al.** Influence of 50 Hz electromagnetic fields in combination with a tumour promoting phorbol ester on protein kinase C and cell cycle in human cells. *Mol Cell Biochem.* 2002; 232: 133–41.
41. **Jou MJ, Peng TI, Yu PZ, et al.** Melatonin protects against common deletion of mitochondrial DNA-augmented mitochondrial oxidative stress and apoptosis. *J Pineal Res.* 2007; 43: 389–403.
42. **Dubocovich ML, Markowska M.** Functional MT1 and MT2 melatonin receptors in mammals. *Endocrine.* 2005; 27: 101–10.
43. **Huan C, Zhou M, Wu M, et al.** Activation of melatonin receptor increases a delayed rectifier K⁺ current in rat cerebellar granule cells. *Brain Res.* 2001; 917: 182–90.
44. **Petit L, Lacroix I, de Coppet P, et al.** Differential signaling of human Mel1a and Mel1b melatonin receptors through the cyclic guanosine 3'-5'-monophosphate pathway. *Biochem Pharmacol.* 1999; 58: 633–9.
45. **Imbesi M, Uz T, Dzitoyeva S, et al.** Melatonin signaling in mouse cerebellar granule cells with variable native MT1 and MT2 melatonin receptors. *Brain Res.* 2008; 1227: 19–25.
46. **Young KA, Caldwell JH.** Modulation of skeletal and cardiac voltage-gated sodium channels by calmodulin. *J Physiol.* 2005; 565: 349–70.
47. **Dai J, Inscho EW, Yuan L, et al.** Modulation of intracellular calcium and calmodulin by melatonin in MCF-7 human breast cancer cells. *J Pineal Res.* 2002; 32: 112–9.
48. **Pandi-Perumal SR, Trakht I, Srinivasan V, et al.** Physiological effects of melatonin: role of melatonin receptors and signal transduction pathways. *Prog Neurobiol.* 2008; 85: 335–53.
49. **Dolezal V, Lisa V, Tucek S.** Effect of tacrine on intracellular calcium in cholinergic SN56 neuronal cells. *Brain Res.* 1997; 769: 219–24.
50. **Vanecek J.** Cellular mechanisms of melatonin action. *Physiol Rev.* 1998; 78: 687–721.
51. **Hazlerigg DG, Morgan PJ, Lawson W, et al.** Melatonin inhibits the activation of cyclic AMP-dependent protein kinase in cultured pars tuberalis cells from ovine pituitary. *J Neuroendocrinol.* 1991; 3: 597–603.
52. **Consales C, Merla C, Marino C, et al.** Electromagnetic fields, oxidative stress, and neurodegeneration. *Int J Cell Biol.* 2012; 2012: 683897.
53. **Lisi A, Ciotti MT, Ledda M, et al.** Exposure to 50 Hz electromagnetic radiation promote early maturation and differentiation in newborn rat cerebellar granule neurons. *J Cell Physiol.* 2005; 204: 532–8.